Atmospheric Pollution Research 11 (2020) 343–356

HOSTED BY

Contents lists available at ScienceDirect

Atmospheric Pollution Research

journal homepage: www.elsevier.com/locate/apr

Chemical characterization of urban PM_{10} in the Tropical Andes

Rasa Zalakeviciute[a,b,*], Yves Rybarczyk[b,c], Maria G. Granda-Albuja[d], Maria Valeria Diaz Suarez[e], Katiuska Alexandrino[a,**]

[a] Grupo de Biodiversidad Medio Ambiente y Salud (BIOMAS), Universidad de Las Americas, calle José Queri y Av. de los Granados / Bloque 7, Quito, EC 170125, Ecuador
[b] Intelligent and Interactive Systems Lab (SI2 Lab) Universidad de Las Americas (UDLA), calle José Queri y Av. de los Granados / Bloque 7, Quito, EC 170125, Ecuador
[c] Dalarna University, Faculty of Data and Information Sciences, 79188 Falun, Sweden
[d] Laboratorios de Investigación, Universidad de Las Américas, calle José Queri y Av. de los Granados / Bloque 5, Quito, EC 170125, Ecuador
[e] Air Quality Monitoring Network, Secretariat of the Environment, Municipality of the Quito Metropolitan District, Quito, Ecuador

ARTICLE INFO

Keywords:
PM10
Urban air pollution
Chemical composition

ABSTRACT

Complex inhalable particles have become one of the main causes to trigger health problems worldwide. While the level of concern depends on the chemical composition of these particles, some regions are poorly studied, particularly, the Andes. In this work, the chemical characterization of atmospheric PM_{10} filter samples, collected between January and October of 2017, was carried out for the first time in the world's highest capital, Quito, Ecuador. This study investigates PM_{10} relation with meteorological variables and criteria pollutants. Average PM_{10} concentrations ranged from 24.9 $\mu g\,m^{-3}$ to 26.2 $\mu g\,m^{-3}$, with some alarming peaks during the episodes of fires and New Year's celebration. The major elements at study sites were Ca, Na, S, Mg, P, K, Fe, Si and Al, while the major water-soluble ion was SO_4^{2-}. Meteorology plays an important role at this complex terrain city. Factor analysis showed natural dust and soil resuspension as the main source of particulate matter. Moreover, two less urbanized sites showed evidence of industrial activities or airport emissions, while the central city site showed a very strong signal of traffic-related pollution. These results are compared with representative cities around the world. As is the case in developing countries, low-quality diesel fuel is recognized for emitting large amounts of heavy metals, resulting in higher levels of those tracers in traffic flow areas. This work demonstrates the problems facing a midsize city, such as the lack of stricter regulations and, thus compromised air quality. This may imply serious respiratory and cardiovascular health effects.

1. Introduction

Harmful air pollution, generated by rapid urban and industrial growth, has become one of the leading causes of premature mortality in the world (Stanek et al., 2011; WHO, 2014). Among atmospheric pollutants, particulate matter (PM) is the most challenging in determining health impacts due to its size, mass concentration and complex chemical composition. PM plays an important role in the biogeochemistry of ecosystems, the hydrological cycle, cloud formation and the atmospheric circulation (Pöschl, 2005). $PM_{2.5}$ and PM_{10}, aerosols with aerodynamic diameters less than or equal to 2.5 μm and 10 μm, respectively, damage the human respiratory and even cardiovascular systems. While elevated levels of PM_{10} are associated with an increase in emergency care visits and hospitalization (James et al., 2018), $PM_{2.5}$ deposits in the lung alveoli and can cause deterioration of cardiopulmonary health (Pope and Dockery, 2006).

PM can originate from several anthropogenic and natural sources, such as road traffic (exhaust and non-exhaust emissions), thermoelectric power plants, cement and paper plants, oil refineries, biomass burning or wildfires, and organic and inorganic particles formed by chemical processes involving precursor gases (Aldabe et al., 2011; Querol et al., 2007; Squizzato et al., 2017). Dust resuspension, sea-salt and construction activities can be other important contributors. As a result, the concentration and composition of PM at a specific location depend on many factors, such as the characteristics of local sources, regional background and meteorological conditions (Rybarczyk and

Peer review under responsibility of Turkish National Committee for Air Pollution Research and Control.
* Corresponding author. Grupo de Biodiversidad Medio Ambiente y Salud (BIOMAS), Universidad de Las Americas, calle José Queri y Av. de los Granados / Bloque 7, Quito, EC 170125, Ecuador.
** Corresponding author.
E-mail addresses: rasa.zalakeviciute@udla.edu.ec, rasa.zalake@gmail.com (R. Zalakeviciute), katiuska.alexandrino@udla.edu.ec, katialexandrino@hotmail.com (K. Alexandrino).

https://doi.org/10.1016/j.apr.2019.11.007
Received 21 July 2019; Received in revised form 20 October 2019; Accepted 2 November 2019
Available online 06 November 2019

Zalakeviciute, 2016).

Composition of PM may include organic and inorganic carbon, chemical elements and water-soluble ions. Metals, such as Ni and V are natural constituents of petroleum, and are found in small concentrations in petroleum-derived products (Korn et al., 2007). They are often correlated with industrial activities due to oil combustion and ship emissions (Viana et al., 2008), and are tracers of very toxic residual oil fly ash (ROFA), responsible for acute changes in cardiac function and excess short-term mortality (Chen and Lippmann, 2009). Fe and Zn also affect human health and are used in the manufacture of fuel tanks and can be transferred to fuels during transport and storage. Furthermore, Ce, Cr, Co, Cu, Pb, Li, Mn, Mo, Ni, Si, Ag, Ti, Sn, W, V, Zn and Zr are introduced in the refinement process or as additives to improve the fuel properties (Du et al., 1997; Pierre et al., 2008; Aucelio and Curtius, 2002). Another highly specific traffic-related element is Sb (brake pads). Anthropogenic and natural sources such as diesel fuel, agricultural, residential, forest and grass burning ash, including Sahara dust, are all great sources of P (Anderson et al., 2010). Moreover, Ca, Mg, Al, Fe, Si, Ti and K have also been attributed to the resuspension of soil dust (Braga et al., 2005). K has also been reported to come from biomass burning (Sánchez-Ccoyllo and de Fátima Andrade, 2002).

On the other hand, water-soluble ions represent a large part of the ion fraction in PM, and are of anthropogenic origin (NO_3^-, NH_4^+, SO_4^{2-}). Those ions are formed in the atmosphere through chemical and/or physical transformations of precursor gases (NO_x, NH_3, SO_2) (Tsai et al., 2012). Other ions include Cl^-, Na^+ (marine origin), Mg^{2+} (exposed soil, unpaved roads and construction activities), K^+ (biomass burning) and Ca^{2+} (mineral contribution) (Moreda-Piñeiro et al., 2015).

Particulate matter source apportionment studies have been performed in different regions of the world, such as North America, Western Europe and Asia (Karagulian et al., 2015). These types of studies are less common in Latin America (Aguilera Sammaritano et al., 2017; Silva et al., 2017; Villalobos et al., 2015), especially in cities of high elevation (reduced density air). There are only a few exceptions, such as Valle de Mexico (2240 m above sea level (m.a.s.l.) (Martínez-España et al., 2018; Molina et al., 2016; Zalakeviciute et al., 2012)) and Bogota (2640 m.a.s.l. (Ramírez et al., 2018)). Nevertheless, the number of cases of asthma and allergy has increased due to the worsening of air pollution in high elevation cities in South America (Bravo Alvarez et al., 2013).

South America is one of the most urbanized continents in the world (United Nations, 2019) with 98% of the cities housing over 100,000 inhabitants, exceeding the air quality recommendations of the World Health Organization (WHO) (Riojas-Rodriguez et al., 2016). Quito, the capital city of Ecuador (2850 m.a.s.l.), is a fast growing urban conglomerate struggling with water (Guerrero-Latorre et al., 2018; Ríos-Touma et al., 2014) and air pollution (Cazorla, 2016; Zalakeviciute et al., 2018, 2017) problems. Some previous studies in Quito showed a correlation between the exposure to air pollution, specifically inhalable particulate matter PM_{10}, and human health (Cevallos et al., 2017; Estrella et al., 2018; Harris et al., 2011). However, the studies on PM chemistry in this city are limited to one study for indoor and outdoor air quality (Raysoni et al., 2017). This implies that there is a lack in knowledge about PM sources and potential health risks.

Therefore, the aim of this work was to perform the chemical characterization of atmospheric PM_{10} (all particulate matter with aerodynamic diameter equal or less than 10 μm, including $PM_{2.5}$) collected in several urban areas in Quito during 2017, using Inductively Coupled Plasma - Optical Emission Spectrometry (IPC-OES) and a spectrophotometer. In addition, the potential emitting sources in the region were identified through Factor Analysis (FA). To the best of our knowledge, this is the first work carried out in the city of Quito addressing the chemical characterization of PM_{10}. Through a comparison with results of other cities around the world, the findings presented herein contribute to understanding and characterizing air pollution in the highest elevation capital city on earth in one of the least studied regions – the Tropical Andes.

2. Materials and methods

2.1. Site description

Quito is one of highest elevation cities in the world, situated at 2850 m.a.s.l. in the Andean mountains (EMASEO, 2011). The city of 2,239,191 inhabitants extends over several terraces that range in elevation between 2700 m.a.s.l. and 3000 m.a.s.l., and descend to the surrounding valleys (2300–2450 m.a.s.l.) (INEC, 2011). This causes serious rush-hour problems due to the limitations imposed on the expansion of the city due to the complex topography. Moreover, high solar intensity, at the equatorial zone, contributes to photochemical smog formation and long-term air pollution problems (Zalakeviciute et al., 2017).

Situated at the equator, the dominating winds vary in their direction during the course of the year (northeast during the Northern hemisphere winter and southeast during the Northern hemisphere summer), but most commonly originate from the east. Due to the terrain complexity, this region is prone to mountain-valley breeze effect responsible for the changes in wind direction during the course of the day, which often may cause a recirculation of urban pollution (Bei et al., 2018; Dong et al., 2017).

The PM_{10} measurement sites were located in three representative areas throughout the city (Fig. 1). A central Site 1 - Belisario (elev. 2835 m.a.s.l., coord.78°29′24″ W, 0°10′48″ S) is the most urbanized site of the study (INEC-DMTV, 2019). A southern valley Site 2 - Los Chillos (elev. 2453 m.a.s.l., coord. 78°27′19″ W, 0°17′48.2″ S) is a site near the industrial activity zone (metallurgic and chemical industries, industrial and auto motor oil and lubricant production, etc.), and is situated 4 km south of a thermal power plant. Finally, the most peri-urban Site 3 - Tababela (elev. 2331 m.a.s.l., coord. 78°20′34.3″ W, 0°11′02″ S) is located in the northern valley district near the international airport.

2.2. PM_{10} sampling and meteorological data

High-volume PM_{10} (all particles with aerodynamic diameter equal or under 10 μm) samplers (Tisch Environmental, INC.; EPA reference method), located on the patios or terraces of buildings, at about 10 m from the ground, were operating with a flow rate of approximately 1.1 $m^3\,min^{-1}$, under actual conditions of temperature and pressure. PM_{10} samplings were carried out between January 1st and October 22nd, 2017 in three study sites (Fig. 1). The 24-h sampling was performed on quartz fiber filters (Whatman, 20.3 cm × 25.4 cm). The frequency of sampling was every sixth day, but only two filters per month, for each sampling site, were selected to carry out the chemical analysis in order to minimize costs (see Table S1, for more detailed information on the dates corresponding to the PM_{10} filters analyzed).

In addition, the data of criteria pollutants ($PM_{2.5}$, CO, O_3, NO_2, SO_2) and meteorological variables (Wind speed, Wind direction, Temperature, Relative humidity, Precipitation accumulation, Solar radiation and Atmospheric pressure) were collected from the air quality network in Belisario, Los Chillos and Tumbaco, described elsewhere (Zalakeviciute et al., 2018, 2017). The two first sites coincide with the PM_{10} filter sampling Sites 1 and 2, while the Tumbaco monitoring station is about 5 km west from the PM_{10} filter sampling Site 3 - Tababela. In all three sites, the criteria pollutants where measured using Thermo Fisher Scientific EPA standard methods, and meteorological variables using Vaisala WXT536 and Kipp & Zonnen instrumentations. The complementary data were compiled as 24-h averages.

$PM_{2.5}/PM_{10}$ fraction analysis data were collected from three available sites also belonging to the city's air quality monitoring network (Guamani, Carapungo and Tumbaco). The real time concentrations of $PM_{2.5}$ and PM_{10} in these monitoring stations were measured using

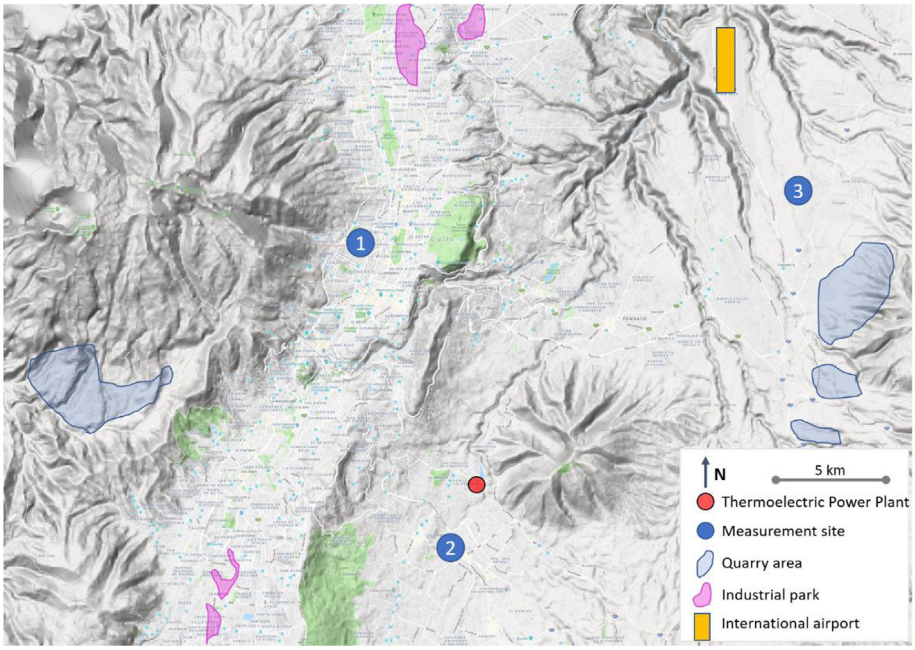

Fig. 1. Map of study sites in the complex terrain of the Metropolitan District of Quito: central Site 1 - Belisario, southern valley Site 2 - Los Chillos and the most rural district Site 3 - Tababela (numbered blue circular markers). Map of Quito was adapted from Google maps.

Thermo Fisher Scientific EPA standard method.

Finally, statistical analyses were performed using Igor Pro 6 (WaveMetrics Inc.) and Microsoft Excel (Microsoft Corporation) software, while maps of Quito were adapted from Google maps.

2.3. Filter conditioning and weighting procedure

Before and after the PM_{10} sampling, the quartz fiber filters were conditioned for 48 h in a room at a constant temperature (20 ± 3 °C) and relative humidity (50 ± 5%). The conditioned filters were weighted in a 0.01 mg sensitivity microbalance (Radwag). Five consecutive weight determinations were performed. After sampling, the filters were stored in zip-lock bags kept at 4 °C to prevent the volatilization of matter from the filter until chemical analyses were performed. Net particulate mass gain was determined gravimetrically by the weight of the filter before and after sampling.

2.4. Sample preparation and chemical analysis

Chemical analyses were performed for filters two days every month for three sites, resulting in a total of 60 filters analyzed. Chemical elements were analyzed by an Inductively Coupled Plasma - Optical Emission Spectroscopy (ICP-OES, Thermo Scientific iCAP 7000 Series). ICP-OES standards (purchased from Sigma Aldrich) were used for the external calibration curve to acquire the concentrations of the following 28 elements: B, Ba, Bi, Cd, Cr, Cu, K, Mn, Ni, Pb, Sr, Ti, Zn, Ca, Fe, Al, Na, Li, Ag, Ga, Mg, V, Te, Se, S, P, Si, and As.

Approximately, 0.0016 m^2 of each loaded filter and blank filters were acid digested (10 mL 65% HNO_3) at 200 °C for 45 min, using a microwave digestion system (MARS 6 - CEM Corporation). The extract solution was filtered using a Whatman No. 2 (125 mm) filter and diluted to a final volume of 50 mL using ultrapure water.

The reliability of the sample analysis was verified by determining the recovery percentage of the extraction method. This verification was carried out by adding the NIST1648a - Urban particulate matter reference material (Sigma-Aldrich) to an unused filter followed by the same extraction procedure as for the samples. The recovery percentages were above 85%, which is considered a good result for analysis validation (Quiroz et al., 2013; Ventura et al., 2014). Limit of detection (LOD) and quantification (LOQ) for each element were calculated as three and ten times the standard deviation of ten independent measurements of blank filters (of each them subjected to the same chemical procedure as the sampled filters) divided by the slope of the analytical curve. The lowest and the highest value of LOD were 9.66×10^{-6} µg g^{-1} (for Sr) and 0.84 µg g^{-1} (for S), respectively, while the lowest and highest values of LOQ were 3.22×10^{-5} µg g^{-1} (for Sr) and 2.79 µg g^{-1} (for S), respectively.

For the water-soluble ion (NO_3^-, NH_4^+ and SO_4^{2-}) fraction in PM_{10}, a 1/32 part of the filter, corresponding to about 0.1 g, was weighted and placed inside an Erlenmeyer flask with 100 mL of Type I water. It was processed in an ultrasound bath for 1 h, subsequently, the sample was filtered through the Whatman filter paper. Specifically, for nitrate analysis, 25 mL of sample was placed in an Erlenmeyer flask. Then 1 mL of 1N Hydrochloric acid was added and left to react for 20 min. After the reaction, it was read in the UV/VIS spectrophotometer at 220 nm (Shimadzu brand) (EPA, 2000). For ammonium analysis, a 25 mL of sample was measured and processed using 1 mL of Phenol Solution, 1 mL of 0.5% Sodium Nitroprusside Solution and 2 mL of oxidizing solution composed of alkaline citrate and sodium hypochlorite, for a duration of 1 h. Afterwards, it was read in the UV/VIS spectrophotometer at 640 nm (Shimadzu brand) (EPA, 1997). And finally, for sulfate analysis 25 mL of sample was placed with 5 mL of Buffer A solution (30 mg $MgCl_2{\cdot}6H_2O$, 5 g $CH_3COONa{\cdot}3H_2O$, 1 g KNO_3, 20 mL CH_3COOH diluted in a total volume of 1000 mL) and 0.5 g of pure Barium Chloride, so that the opalescence of the sample could be observed. The sample was stirred for 1 min and read at 420 nm on the UV/VIS spectrophotometer (Shimadzu brand).

2.5. Factor Analysis

A Factor Analysis (FA) was carried out to describe the original variables (i.e., the chemical element concentration) according to a reduced number of orthogonal factors (also called eigenvectors). This analysis allowed us to evaluate and to identify the PM_{10} polluting sources in the city of Quito. The FA algorithm searches for the best axes to project the samples that minimize the loss of information (or variability) for the cloud of data points. This FA enables us to visualize in two dimensions (i) the correlation among the variables and (ii) between

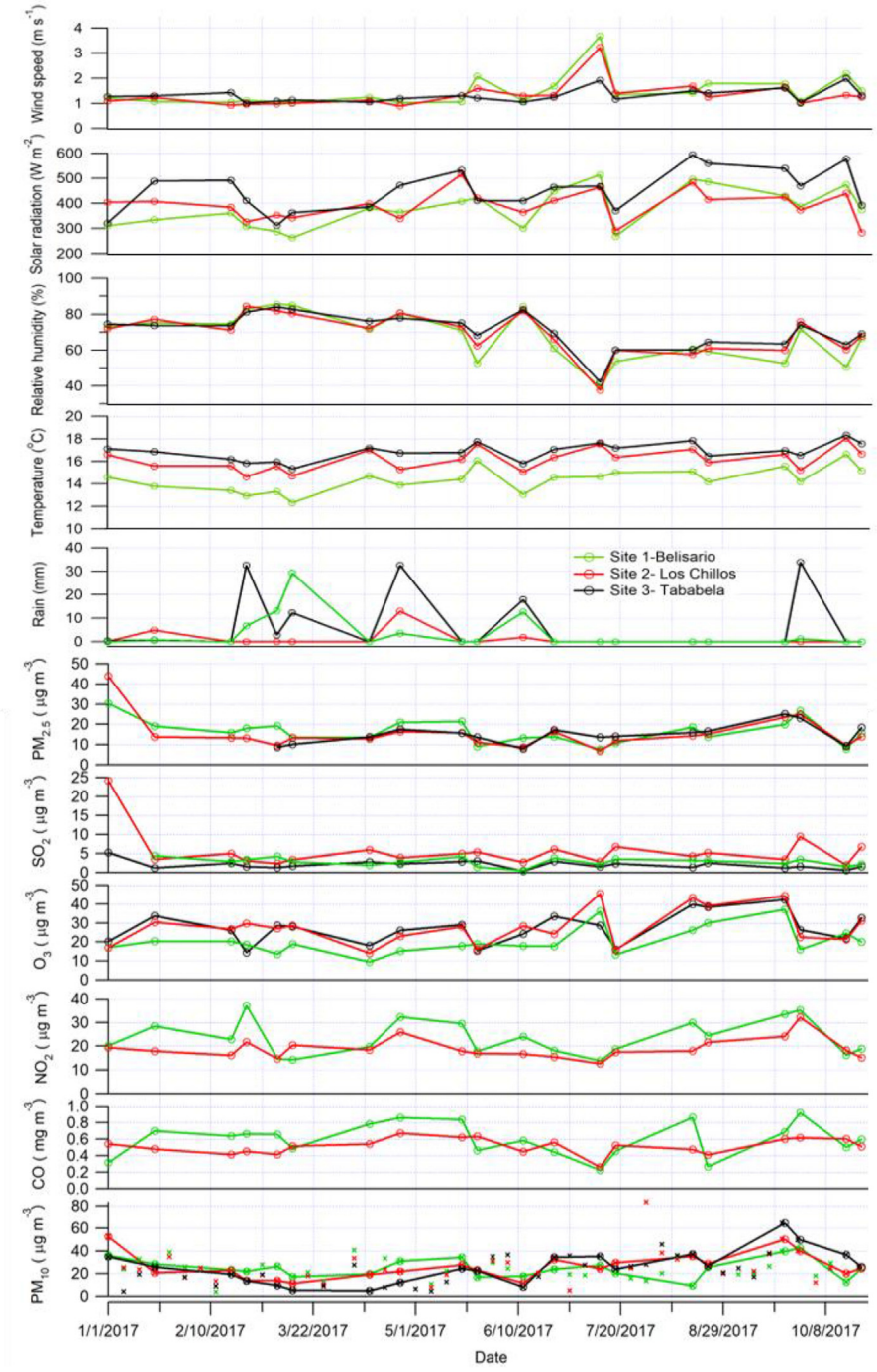

Fig. 2. Meteorological (Wind speed, Solar radiation, Relative humidity, Temperature and Rain) and chemical ($PM_{2.5}$, SO_2, O_3, NO_2, CO and PM_{10}) variables for three sites in Quito, Ecuador from January to October 2017. Round marker lines represent days of chemical analysis, and cross markers represent all days of collected PM_{10} samples.

the variables and the factors.

In practice, the matrix of the source data, represented by p variables (here p = 15) and n observations (here n = 19), is transformed into a factor matrix, represented by the two factors (e.g., F1 and F2) that explain the maximum percentage of variability of the original data. Consequently, the samples can be explored in a new variable space defined by the factors, or dimensions, which are orthogonal, uncorrelated and a linear combination of the standardized variables (x_p).

Once the FA is performed, two parameters are relevant to interpret the results. First, it is the vector magnitude that represents the variability of the variables (the longer the vector, the higher the percentage of variability explained by the space transformation). And second, it is the angle between the vectors which expresses the correlation between the variables (the smaller the angle, the higher the correlation).

Here, three FA were run, one for each sampling site (Belisario, Los Chillos and Tababela). First, an optimal number of parameters was tested to not lose the representation of the possible sources (i.e. get eigenvalues as high as possible). Finally, 15 metals were chosen: Na, Ca, Al, Fe, Mg, Mn, Ba, Ni, V, Cr, Cu, Zn, Pb, Cd and Sr. Moreover, total PM_{10}, NO_3^-, NH_4^+, SO_4^{2-}, relative humidity and temperature were included as supplementary quantitative parameters, to provide additional variables to interpret the results. The number of parameters was

limited to 15 chemical elements and 6 supplementary variables in order to sustain the precision of the model, by increasing the percentage of explanation of each dimension. We wanted to explain around 60% of the variability. From the 20 original observations, the January 1st, 2017 data was removed from the analysis, because of the unrepresentative high values in PM_{10} that can be considered as outliers. By combining the results of this analysis and the scientific knowledge, it is possible to group metals into different clusters of pollution sources (natural vs. anthropogenic), which are represented in a bidimensional space. Each axis is supposed to explain a different origin of contamination. The analysis was carried out through a program in R by using the libraries 'FactoMineR' and 'factoextra' and was developed in the software application RStudio.

2.6. Comparative analysis with other cities

In order to compare the findings of this study with those of other cities, two comparative analyses were performed. First, the comparison of the concentration of PM_{10} and chemical elements in Quito with the studies of other 11 cities in the world was performed. Then, the impact of some parameters, such as year, population and elevation, on the characteristics of urban pollution was investigated. This analysis consisted of determining the representation of the elements in terms of a fraction of the total mass of PM_{10}. To do this, the average concentration of the chemical elements was divided by the mean value of PM_{10} for the respective site. This normalization allowed us to apply a certain correction to the heterogeneity of the collected data (different year of the study and variation in population size) and make possible the comparison between the cities. In order to identify the impact of these parameters on the proportion of natural-related versus anthropogenic-related (traffic and industry) sources of contamination, first, the concentration of each source group was calculated from the average value of all the characteristic elements of the group. Then, the ratio of each group was obtained by dividing the value calculated in the previous step by the average concentration of the four groups. For this step, it was preferred to use the average instead of the sum to minimize a possible bias induced by missing values.

3. Results and discussion

3.1. PM_{10} concentrations and meteorology

In this section, the correlation between PM_{10} concentrations and meteorological variables and criteria pollutants ($PM_{2.5}$, SO_2, O_3, NO_2, and CO) is investigated. Visual demonstration in Fig. 2 is supported by a Pearson analysis (Tables S2–S4). The Pearson analysis also includes the concentrations of chemical elements and water-soluble ions for further discussion in section 3.3.

Fig. 2 shows 24-h cumulative PM_{10} concentrations during the period of the study: all the collected filter samples (cross markers), and the filters that have been analyzed for chemical composition (round markers connected by line). Although daily average PM_{10} concentrations do not violate national air quality standards ($100\,\mu g\,m^{-3}$), in a few occasions during the year, the WHO recommendation for 24-h ($50\,\mu g\,m^{-3}$) is exceeded. Most of those peaks coincide with the New Year's celebrations and regional fire episodes. For example, a large area of forest south of the city burned in July 2017, doubling the PM_{10} concentrations for that period in the southern valley Site 2 - Los Chillos (Fig. 2, red cross markers). Furthermore, the overall average of PM_{10} concentrations exceeds health recommendations for annual PM_{10} levels ($20\,\mu g\,m^{-3}$) at all study sites (Table 1). Average PM_{10} concentration (Table 1) was the lowest in the central Site 1 - Belisario ($24.9 \pm 9.2\,\mu g\,m^{-3}$) and the highest in the southern valley Site 2 - Los Chillos ($26.2 \pm 11.1\,\mu g\,m^{-3}$). However, not counting the days with peak values (due to festivities and fires), the central Site 1 - Belisario showed higher overall concentrations of PM_{10} (data not shown here). The least urbanized Site 3 - Tababela, in close proximity to the international airport, showed the lowest variability in PM_{10} concentrations ($25.7 \pm 4.7\,\mu g\,m^{-3}$).

Fig. 2 also shows 24-h average wind speed, relative humidity, temperature, daytime (6:00–18:00) average solar radiation, and 24-h cumulative precipitation at three sampling sites. During the study period, average temperature varied a little: $14.4 \pm 1.1\,^{\circ}C$ at central Site 1 - Belisario, $16.2 \pm 0.9\,^{\circ}C$ at Site 2 - Los Chillos and $16.9 \pm 0.8\,^{\circ}C$ at Site 3 - Tababela. Meanwhile, precipitation patterns were more variable. Cumulative daily precipitation ranged from 0 mm to over 30 mm. Overall, the rainiest site was Tababela (133 mm), followed by Belisario (67 mm) and Los Chillos (20 mm). Wind speed was greater during the summer months (dry season, June–August) at $1.64 \pm 0.65\,m\,s^{-1}$, compared to the rest of the year ($1.17 \pm 0.23\,m\,s^{-1}$) (Fig. 2).

The days with high PM_{10} concentration were associated with increased ambient temperature, high ventilation (dust suspension), absence of precipitation and low relative humidity (Fig. 2) (Braga et al., 2005; Quiterio et al., 2004; Sánchez-Ccoyllo and de Fátima Andrade, 2002). Solar radiation correlates with ambient temperature and wind speed, which in turn causes an increase in PM concentrations, due to dust suspension or pollution transport (Tables S2–S4). It can be observed that this depends on the site. In the case of central and traffic-busy Site 1 - Belisario, an increase in wind speed causes an increase in pollution (pollution transport), while in other sites it causes dust resuspension or ventilation effect (Fig. 2 and Tables S2–S4).

Fig. 2 also shows 24-h average concentrations of criteria pollutants ($PM_{2.5}$, SO_2, O_3, NO_2, and CO) during the study period at study sites. It is observed that peak SO_2 and PM concentrations coincide on January 1st, 2017 at all sampling sites with the available data. This is attributed to the New Year's celebrations, such as fireworks and massive burning of traditional dummies in the streets. An increase in gaseous and particulate pollution during the firework events is a worldwide recognized phenomenon raising health concerns (Do et al., 2012; Greven et al., 2019; Licudine et al., 2012; Steinhauser et al., 2008).

It is observed in Tables S2–S4, that there is a significant positive correlation between PM_{10} and $PM_{2.5}$ at all sites. Furthermore, PM_{10}, $PM_{2.5}$, NO_2, CO and SO_2 concentrations often correlate with each other. However, the high correlation of PM with CO and NO_2, at the central Site 1 - Belisario, suggests motor vehicle exhaust pollution contribution. It is worth noting that the correlation of $PM_{2.5}$ with CO and NO_2 was higher than the correlation of PM_{10} with CO and NO_2. This implies that the emissions of these gaseous pollutants are accompanied by the emissions of fine particles, as it has been demonstrated in previous works (Yangyang et al., 2015). At Site 2 - Los Chillos a strong significant correlation of PM with SO_2 and NO_2 indicates the influence of thermoelectric plant on local pollution. Finally, at Site 3 - Tababela a significant correlation between O_3 and $PM_{2.5}$ is observed. O_3, as an oxidant, can change the concentration of free radicals in the atmosphere, thus if O_3 concentration increases, the formation of particulate matter can be strengthened (Jia et al., 2017; Xiao et al., 2011).

The $PM_{2.5}/PM_{10}$ ratio was analyzed for a number of monitoring network sites (with available information on both particle size ranges). $PM_{2.5}/PM_{10}$ ratio varied from 0.45 to 0.89 in Quito, comparing well with other studies (Ho et al., 2003; Querol et al., 2004; Sharma and Maloo, 2005). These findings advocate the importance of studying the chemical composition of PM_{10}, due to health implications, especially because of the significant fraction of smaller particles in PM_{10}.

Finally, the analysis of wind was performed for all three sites (Fig. 3). Foremost, the effect of local complex topography can be observed for Sites 1 and 2. Wind speed is very low on the side of the mountain and is dominating to the directions of open paths of the mountain terrain (Fig. 3a and c). Fig. 3a shows that at Site 1 - Belisario the dominating winds come from the southeast, dictated by the geography of the city. Surrounded by the two mountain ranges from the west and the east, wind sweeps all the air pollution produced in the

Table 1
Chemical analysis of PM_{10} for the three sampling sites in Quito.

Site 1				Site 2			Site 3		
Belisario				Los Chillos			Tababela		
Element	Ave.	Min.	Max.	Ave.	Min.	Max.	Ave.	Min.	Max.
PM_{10} (μg m^{-3})	24.9	9.2	42.4	26.2	11.1	52.6	25.7	4.7	64.6
μg m^{-3}									
Ca	7.617	3.440	11.220	6.552	0.829	9.292	7.809	4.094	11.953
Na	4.786	2.730	12.149	3.910	0.462	6.427	4.324	2.991	5.924
S	1.207	0	2.564	1.113	0	2.707	1.014	0	2.724
Mg	1.825	0.808	2.726	1.556	0.198	2.217	1.894	0.954	2.956
P	0.930	0	2.004	0.910	0	1.915	0.908	0	1.837
K	0.728	0.211	3.209	0.408	0.044	0.768	0.387	0.191	0.563
Fe	0.444	0.222	0.992	0.363	0.0719	0.784	0.412	0.0916	0.780
Si	0.255	0	0.726	0.196	0	0.498	0.228	0	0.619
Al	0.382	0.161	1.046	0.470	0	1.884	0.913	0.125	2.163
Ba	0.242	0.089	0.841	0.170	0.007	0.442	0.138	0.0321	0.433
SO_4^{2-}	3.223	1.124	7.349	2.639	0.899	5.569	2.340	0.912	5.616
NO_3^-	0.397	0.178	0.913	0.398	0.119	0.705	0.332	0.077	0.601
NH_4^+	0.155	0.029	0.583	0.069	0.016	0.183	0.068	0.015	0.150
ng m^{-3}									
Zn	121.283	16.675	431.770	102.836	10.509	278.367	65.136	15.301	182.087
B	113.798	0	419.688	35.211	4.965	106.894	38.491	3.151	146.405
Cu	97.770	23.527	268.520	200.073	9.925	863.635	53.511	15.119	164.123
Cr	95.440	2.492	1158.264	9.258	0.736	28.193	23.311	2.421	117.046
Ga	73.775	0	150.011	48.423	0	154.468	57.339	0	121.652
Sr	56.754	16.290	165.221	33.936	3.424	65.594	32.164	16.319	46.718
Mn	41.710	21.199	68.844	32.454	3.551	59.071	31.094	14.820	78.126
As	5.936	0	5.936	0.4782	0	2.069	1.922	0.451	2.880
Pb	19.570	0.591	83.664	23.854	2.489	107.911	19.797	1.779	89.067
Te	9.630	0	36.135	11.269	0	56.080	12.126	0	47.868
Ni	14.654	0	126.828	7.708	0.210	25.412	2.836	0	7.494
Ag	9.578	0	25.381	11.644	0	44.438	17.068	0	55.096
Se	9.630	0	36.135	7.432	0	35.770	9.129	0	30.360
Bi	0.942	0	14.644	0.546	0	6.833	0	0	0
V	5.006	0	17.211	10.119	0	59.842	5.404	0	11.952
Cd	2.909	0.316	14.145	1.522	0.070	5.825	2.100	0.250	7.445
Li	0.142	0	2.833	0.269	0	2.289	0.424	0	4.2
Tl	ND	ND	ND	0.0767	0	1.534	0.0319	0	0.6

urban canyon towards this site. As per terrain complexity, the effect of mountain-valley breeze is responsible for wind direction changes during the course of the day. This may cause a recirculation of urban pollution (Bei et al., 2018; Dong et al., 2017). A deeper daily analysis of the wind direction shows a dominant easterly wind during the daytime (valley breeze) and weaker northerly and northwesterly (mountain breeze) winds at night (Fig. 3b). This change in wind direction correlates with more urban pollution originating from the south and the southeast. Strong north winds are also common at Site 1, as the trend winds change their direction during the windiest summer months (June–August). Similar tendencies are observed in other study sites. In the case of Site 2 - Los Chillos, winds are common from the east and the southeast of the valley during the day, while night winds originate more from the northern direction (thermoelectric power plant) (Fig. 3c). As a result, even at night, the concentrations of fine particles may increase (Fig. 3d). Finally, at more open topography Site 3 - Tababela the dominating winds come from the east, the north (international airport) and the northeast, following the direction of the trend winds (Fig. 3e and f).

3.2. Chemical analysis of PM_{10}

Table 1 summarizes the mean, minimum and maximum concentration of the chemical elements found in the PM_{10} samples in the three sites. It is observed that the major elements in the three sampling sites are Ca, Na, S, Mg, P, K, Fe, Si and Al, with Ca being the most abundant in all sites, indicating that soil and dust resuspension prevails in this region. When compared with the less urbanized Sites 2 and 3, central Site 1 - Belisario presents higher concentrations of Zn, B, Ba, Cr, Sr, Mn, Ni and Cd, all associated with anthropogenic emissions.

Southern valley Site 2 - Los Chillos presents a much higher concentration for Cu, Pb, Te, Se and V, which are elements mainly related to burning of fossil fuels or industrial activities (Almeida et al., 2017; Karagulian et al., 2015; Viana et al., 2008, 2007; Watson and Chow, 2001). This site is within an area of increased industrial activity, where a thermoelectric power plant, known to burn diesel, fuel-oil and reduced crude oil, is located (Zalakeviciute et al., 2017). On the contrary, the most rural Site 3 - Tababela presents higher values for natural tracers Al, Mg, Na, Si and Ca, if compared to the other two sampling sites.

It is worth noting that Pb is detected in all sampling sites exhibiting similar concentration at Sites 1 and 3, while at Site 2 the concentration is higher. Howbeit, the Pb concentration was below the annual WHO guideline of 0.5 μg m^{-3} at all sampling sites. This heavy metal was banned in Ecuador since 2000, so its presence in these areas could be related with non-exhaust emissions from road traffic (Lough et al., 2005; Thorpe and Harrison, 2008; Young et al., 2002). Moreover, it has been indicated in literature that Pb persists for several decades in soil/dust (Shen et al., 2016), so its presence could also be due to the resuspension of the earlier vehicular emissions.

In addition, as expected, during the events of fires in the region, the biomass-burning tracer K showed an increase in concentrations at all sites. Moreover, it was observed that the concentration of metals present in fireworks, such as Cu, Mg, Sr, Pb, Cr and Na (Do et al., 2012; Greven et al., 2019; Licudine et al., 2012; Phantom Fireworks, 2019; Steinhauser et al., 2008), exhibited a jump on the 1st of January 2017 (not shown here). The latter two metals exhibited those concentration peaks only on the 1st of January, while the others had some other peaks

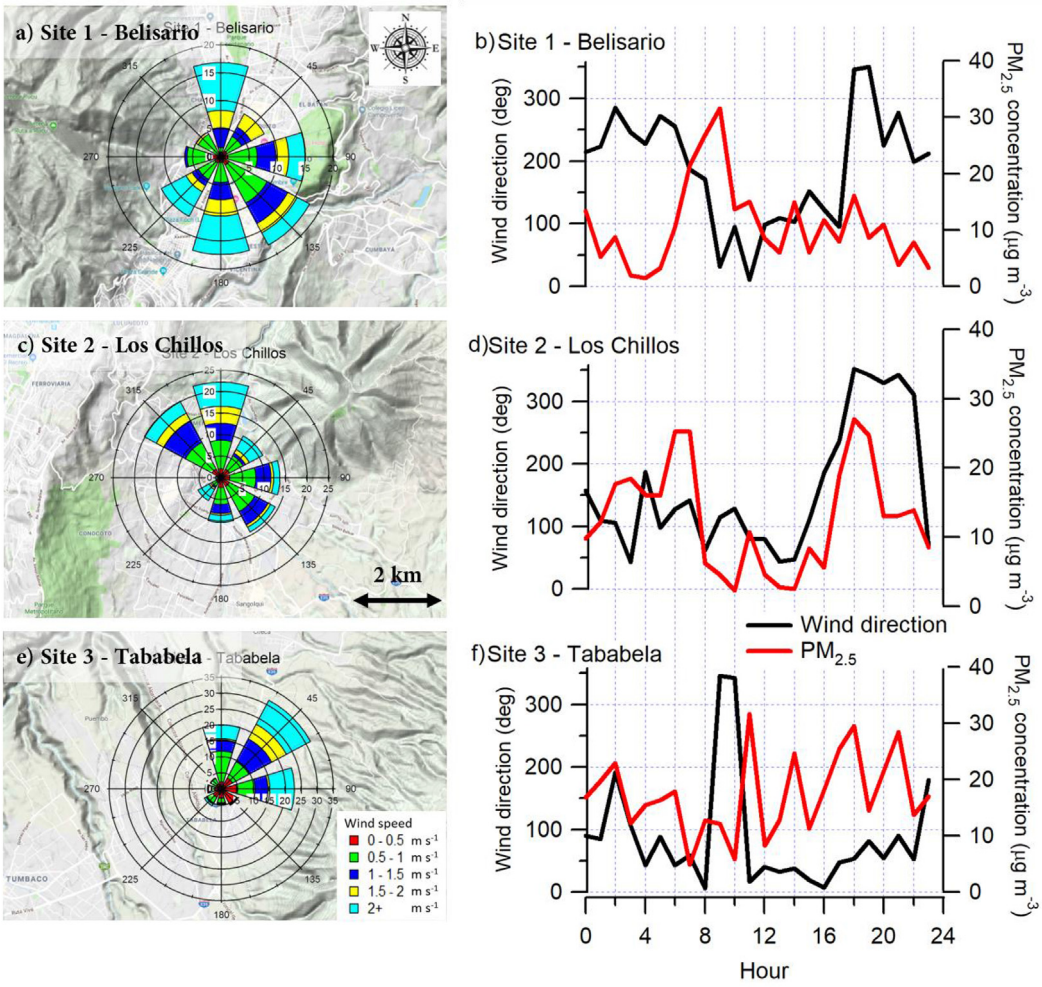

Fig. 3. Wind roses for the study sites: a) Site 1- Belisario, c) Site 2- Los Chillos and e) Site 3- Los Chillos. And hourly wind direction and $PM_{2.5}$ concentration measurements for selected days for the study sites: b) Site 1- Belisario, d) Site 2- Los Chillos and f) Site 3- Los Chillos.

throughout the year.

Unfortunately, it is found that the mean concentration of toxic heavy metals in Quito, like Cr and As, violate the health recommendations of 0.2 ng m^{-3} and 0.57 ng m^{-3}, respectively (Licudine et al., 2012). For example, average concentrations of As exceed health recommendations by up to 10 times and Cr by up to 475 times, depending on the site. In both cases, the concentration of these heavy metals is the highest in the central Site 1 - Belisario, raising serious health concerns for the population (Gibb et al., 2000), especially densely populated and transited in this part of the city. Moreover, it is identified that the concentration of Ni exceed the US-EPA standard value of 0.24 ng m^{-3} (Quiterio et al., 2004), mainly in Site 1 - Belisario, where Ni concentration is 61.25 times higher than the standard value. This metal is mainly associated with oil burning, fossil fuel use, and emissions from industrial and stationary sources. Moreover, it can also be emitted from vehicle exhaust as it is used as an additive in fuels (López et al., 2005). As previously mentioned, this site is downwind from a big part of the city, north of residential, traffic and industrial activities.

Table 1 also shows the concentrations of water-soluble ions. SO_4^{2-}, NO_3^- and NH_4^+ are secondary aerosols formed through the oxidation of SO_2 and NO_x (Kai et al., 2007) and the reaction between NH_3 and acidic species present in either the gas or aerosol phase (Zhou et al., 2016). SO_2 and NO_x can be converted to SO_4^{2-} and NO_3^-, respectively: (i) through atmospheric photochemical changes that convert directly SO_2 and NO_x into SO_4^{2-}, NO_3^-; (ii) through the reaction with H_2O to acid which are oxydized; and (iii) through heterogeneous reactions that occur on the aqueous surface layer of preexisting particles where SO_2 and NO_x react with O_3, H_2O_2 or OH to form SO_4^{2-} and NO_3^- (Ding and Zhu, 2003; Wrzesinsky and Klemm, 2000; Yao et al., 2002). The latter pathway is much more efficient than homogeneous formation in the atmosphere, the efficiency of which increased with increasing humidity when humidity increases (Li-Jones and Prospero, 1998; Yao et al., 2002). It is observed that the SO_4^{2-} concentration is higher than the rest of ions for all the studied sites, being higher in the Site 1 - Belisario than in the other two sampling sites. This fact could strongly suggest contribution from combustion emissions. It is observed in Table S3 that, in Site 2 - Los Chillos, NO_3^- is significantly related to relativity humidity (R = 0.54), while in Site 3 - Tababela a significant correlation between SO_4^{2-} and rain exist (R = 0.52). The latter correlates well with relativity humidity (R = 0.46) (Table S4), which may indicate that the formation of SO_4^{2-} and NO_3^- occur mainly by path (iii) in these sites. Moreover, the positive correlation between SO_4^{2-} and rain in Site 3 could also suggest an indirect effect of precipitation on reduced wind speeds (R = 0.46), and thus reduced pollution ventilation. This is further supported by even better correlation between SO_4^{2-} and wind speed (R = −0.59).

It is worth mentioning that NO_3^- strongly significantly anticorrelated with atmospheric pressure (R = −0.66) in the most urbanized Site 1 - Belisario (Table S2). Since high pressure system forms in the region during the summer months (June–August), with reduced traffic activity, and significantly stronger winds, this could explain in

Table 2
Loads and explained variance (percentage and eigenvalue) of each element for the four most significant FA dimensions in Site 1 - Belisario.

Element	Factor 1	Factor 2	Factor 3	Factor 4
Ba	0.67	0.27	−0.08	0.67
Sr	0.93	0.17	0.23	−0.16
Cd	0.94	−0.20	0.12	−0.16
Cr	0.54	0.10	0.03	−0.39
Cu	0.87	0.22	0.06	−0.04
Mn	0.66	0.58	0.13	−0.13
Pb	0.77	−0.25	0.03	0.08
Zn	0.77	0.33	−0.14	0.44
Ni	0.79	−0.43	0.24	−0.15
V	−0.29	−0.32	0.85	0.20
Ca	0.04	0.83	0.36	−0.11
Fe	−0.38	0.50	0.43	0.13
Al	−0.25	0.52	0.52	−0.13
Na	−0.22	0.68	0.18	−0.18
Mg	0.12	0.77	0.25	−0.18
Eigenvalue	**5.96**	**2.87**	**2.45**	**1.20**
Variance (%)	**39.76**	**19.11**	**16.37**	**7.97**
Cumulative variance (%)	**39.76**	**58.87**	**75.23**	**83.21**

Table 4
Loads and explained variance (percentage and eigenvalue) of each element for the four most significant FA dimensions in Site 3 - Tababela.

Element	Factor 1	Factor 2	Factor 3	Factor 4
Ba	0.04	0.92	−0.36	−0.07
Sr	0.90	−0.16	−0.37	0.00
Cd	0.87	0.13	0.18	−0.20
Cr	0.36	0.02	0.55	−0.58
Cu	0.62	−0.07	0.01	−0.29
Mn	0.71	−0.25	−0.31	0.17
Zn	0.40	0.88	0.11	−0.12
Pb	−0.12	0.44	0.43	0.60
Ni	0.81	−0.03	0.51	0.12
V	0.75	0.28	0.43	0.17
Ca	0.93	−0.11	−0.20	−0.09
Fe	0.69	0.02	−0.02	0.66
Al	0.94	0.01	0.21	0.00
Na	0.57	−0.25	−0.48	0.22
Mg	0.95	−0.11	−0.19	−0.07
Eigenvalue	**6.96**	**2.96**	**1.87**	**1.15**
Variance (%)	**46.39**	**19.77**	**12.44**	**7.66**
Cumulative variance (%)	**46.39**	**66.15**	**78.59**	**86.25**

the drop of NO_3^- concentrations due to ventilation effect. Similarly, at Site 2 - Los Chillos NO_3^- negatively correlates with wind speed ($R = -0.46$), also pointing to ventilation effect.

3.3. Factor analysis of elements

In order to identify the sources of PM_{10} emissions, Factor Analysis (FA) was performed for each sampling site. For this analysis, 15 elements were selected, among the 28 analyzed. Factors with eigenvalues > 1 were considered relevant. Four factors were identified, explaining around 85% of the data variability for each sampling site (Tables 2–4). Additionally, a biplot, based on the first and second components of the FA for element concentrations, was represented for each study site (Fig. 4). These two factors explain the majority (about 60% in all sites) of the data variability. In this plot, PM_{10} concentration, a few selected meteorological parameters (temperature and relative humidity) and ion concentrations were added as supplementary variables, based on the best trial results. This was done in order to assess the correlation of these additional parameters with the variable considered in the FA (concentration of chemical elements) and, consequently, to complement the explanation of the results. In Fig. 4 the elements were split into industry (blue markers), traffic (red markers), mixed traffic/industry (purple markers) and natural (green markers) sources based on the results from Tables 2–4 and literature. Moreover, in order to support the conclusions obtained from FA, the Pearson correlation analysis, mentioned previously in section 3.1, was used (Tables S2–S4).

Table 3
Loads and explained variance (percentage and eigenvalue) of each element for the four most significant FA dimensions in Site 2 - Los Chillos.

Element	Factor 1	Factor 2	Factor 3	Factor 4
Ba	−0.14	0.59	0.78	−0.13
Sr	0.95	0.16	−0.06	0.20
Cd	0.82	−0.34	0.16	0.25
Cr	0.60	−0.35	0.05	0.32
Cu	0.20	0.16	0.30	0.61
Mn	0.77	0.44	−0.27	−0.07
Pb	0.87	−0.35	0.22	−0.02
Zn	0.37	0.01	0.85	0.22
Ni	0.77	−0.35	0.19	−0.40
V	0.77	−0.31	0.17	−0.45
Ca	0.47	0.74	−0.38	0.08
Fe	0.33	0.66	−0.17	−0.31
Al	−0.10	0.21	0.19	0.28
Na	0.22	0.82	−0.35	−0.24
Mg	0.50	0.72	−0.36	0.12
Eigenvalue	**5.85**	**3.12**	**2.48**	**1.20**
Variance (%)	**38.99**	**20.79**	**16.53**	**7.99**
Cumulative variance (%)	**38.99**	**59.78**	**76.30**	**84.29**

In the most urbanized central Site 1 - Belisario, Factor 1 is dominated by Ba, Sr, Cd, Cr, Cu, Mn, Pb, Zn and Ni, which suggest the influence of anthropogenic sources (vehicular emissions and industries) (Table 2, Fig. 4a). Because there is a high traffic flow in this site, instead of industrial activities, the emissions are mainly attributed to road traffic, specifically from non-exhaust emissions, such as wear of tire tread and brake linings (Thorpe and Harrison, 2008). This can be supported by Fig. 4a where it is observed that traffic tracers Ba and Sr overlap with the mixed traffic/industry cluster formed by Cr, Zn, Pb, Cu, Cd and Mn (Viana et al., 2008, 2007; Watson and Chow, 2001). All of them show a strong confidence level indicated by the large magnitude of the eigenvectors (see Fig. 4a) and high Pearson correlation coefficients (see Table S2). Factor 2 has high loading for Ca, Fe, Al, Na and Mg also forming a cluster (Fig. 4) that may be explained by natural sources, such as dust and soil particles (Belis et al., 2013; Karagulian et al., 2015). On the other hand, Fig. 4a shows that V has a low confidence level (small vector length) and this is because this heavy metal is better described by Factor 3 rather than Factor 1 or 2 (see Table 2). Finally, Pearson analysis (Table S2) shows the importance of wind speed in pollution transport (K), and the importance of temperature increase in resuspension of natural PM components (Ca, Fe, Al, Mg). This can be explained by the effect of surface warming on turbulence. The anticorrelation between criteria pollutants and non-exhaust motor vehicle tracers indicates different conditions for forming part of PM. While the latter require more ventilation, the former require more stagnant atmospheric conditions.

In the Southern valley Site 2 - Los Chillos, Factor 1 includes Sr, Cd, Cr, Mn, Pb, Ni and V, and may be associated with the various industrial activities in the surroundings of the monitoring station, such as steel industry and thermoelectric power plant (Table 3, Fig. 4b). The highly intercorrelated industrial tracers (V and Ni) are encompassed in the cluster formed by the mixed traffic/industrial tracers (Fig. 4b), which could confirm that this zone has industrial activity that contribute to the metal composition in the PM_{10}. Steel industry has been reported to emit Mn, Ni and Cr (Braga et al., 2005; Quiterio et al., 2004), while thermoelectric power plant is known to emit Cd, Cr, Pb, Ni and V (Pastrana-Corral et al., 2017; Rotatori et al., 2003). This is further supported by SO_2 correlation with Mn, Ni, Zn and V (Table S3). Factor 2 is represented by the natural related elements Ca, Fe, Na and Mg, forming a cluster (Fig. 4b). These elements are positively correlated with each other and with total PM_{10} and, as in the case of Site 1, with

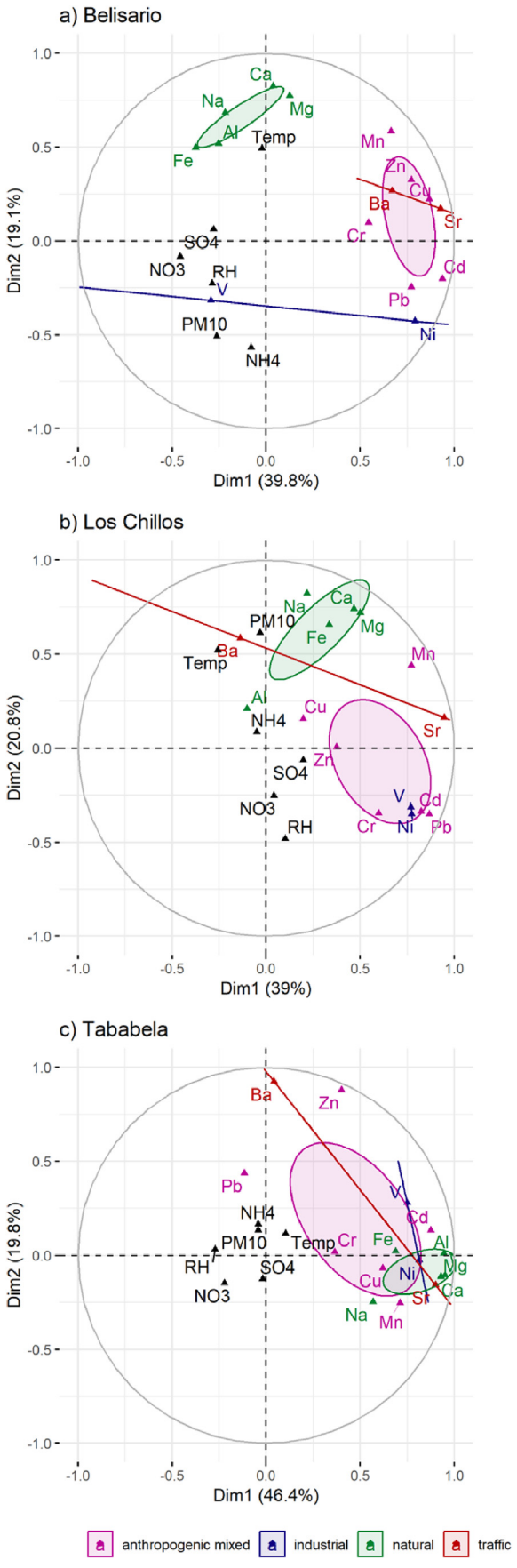

Fig. 4. Biplots based on the first and second components of the FA for element concentrations in the PM_{10} filters at: a) Site 1- Belisario, b) Site 2- Los Chillos, c) Site 3- Tababela. The supplementary variables NH4, SO4, NO3, RH and Temp stand for ammonium, sulfate, nitrate, relative humidity and temperature, respectively. For better clarity, the eigenvectors are represented by dots.

temperature and wind speed, indicating the effect of resuspension (Table S3). Factor 3 has significant loadings for Ba and Zn. These metals have been identified to be present in brake dust samples (Iijima et al., 2007; Lough et al., 2005; Sternbeck et al., 2002; Thorpe and Harrison, 2008). Moreover, Zn has also been associated with tire dust (Fergusson and Kim, 1991; Sadiq et al., 1989; Smolders and Degryse, 2002; Thorpe and Harrison, 2008). This indicates, that there is a third source related to road traffic. Finally, the fourth factor is represented by Cu, which is a tracer for smelting furnace burning, diesel combustion and break lining wear (Dai et al., 2015).

In the most peri-urban district Site 3 - Tababela, the FA reflects a complex pollution pattern originated from various sources. Factor 1 explains almost half (46.4%) of the variance, and is loaded with Sr, Cd, Cu, Mn, Ni, V, Ca, Fe, Al, Na and Mg which are elements from natural and anthropogenic sources (Table 4). This might suggest that soil in this region is enriched with a sedimentation of transported particles, due to the fact that there are not many industrial nor traffic activities in this area. This is supported by Fig. 4c that shows that the traffic and industrial tracers are encompassed in two overlapping clusters. Likewise, Pearson correlation analysis shows a wide array of parameters that correlate with each other, in contrast to other sites (see Table S4). A significant correlation of solar radiation and temperature with multiple industrial and natural tracers points to resuspension of those components. Furthermore, this zone contains the international airport, which might cause very different trends in the presence of heavy metals in the filter samples (see Fig. 4c). Aircraft jet engines are known to emit metal particles such as Pb, Zn, V, Cu (Boyle, 1996), Ba and Al (Fordyce and Sheibley, 1975) due to engine erosion and the combustion of fuel containing trace metal impurities.

Regarding to the water-soluble ions (Fig. 4), they tend to be grouped away from the primary elemental components in the case of Site 1 - Belisario (Fig. 4a). This confirms that all analyzed ions are originated in a different manner. On the other hand, for Site 2 - Los Chillos and Site 3 - Tababela, the cluster of these ions is located very close to the center of the graph, indicating a limited reliability of the explanation of these data in this factorial space (Fig. 4b and c, Tables S3 and S4).

3.4. Comparison with other cities

The concentrations of PM_{10}, some chemical elements and water-soluble ions found in the present study were compared to the results of a number of available studies performed in other cities around the world (see Table 5). The comparison includes cities in: (i) Latin America, such as Cienfuegos (Cuba), Chillan (Chile), Cordoba and Buenos Aires (Argentina), Rio de Janeiro (Brazil), Bogota (Colombia) and Mexico City (Mexico); (ii) Europe, such as Palermo (Italy) and Athens (Greece); and (iii) Asia, such as Kanpur (India) and Hong Kong (China). Although the cities encompass a wide range of population sizes (146,701–18,457,000 inhab.) and a variety of elevations (14-2850 m.a.s.l.), the characteristics of the sites in these studies compare well with those in this work, i.e., urban and/or industrial areas. Since the reviewed studies vary by the year of investigation, the normalization techniques described in section 2.6 were applied to mitigate the effects of the evolution of fuel quality, industry regulations, rapid industrialization and motorization of the cities.

It can be observed in Table 5 that, the concentration of metals associated with natural sources, such as Mg, Ca and Na, was found to be higher in Quito than in other cities around the world. This could be due to different factors, such as the chemistry composition of natural

Table 5
Concentration (μg m^{-3}) of PM_{10}, elements and water-soluble ions in Quito compared with other cities around the world.

	Chillan (Chile)[b]	Cienfuegos (Cuba)[a]	Palermo (Italy)[c]	Cordoba (Argentina)[d]	Quito[l] (Ecuador)	Kanpur (India)[f]	Athens (Greece)[g]	Rio de Janeiro (Brasil)[h]	Hong Kong (China)[i]	Bogota (Colombia)[j]	Buenos Aires (Argentina)[e]	Mexico city (Mexico)[k]
Year	2001–2003	2015–2016	2005	2009–2010	2017	2002–2003	2001–2002	2009	2000–2001	2008	1998–1999	2000
Population	146,701	150,404	673,735	1,391,000	2,239,191	2,715,555	3,187,000	6,320,446	6,730,000	7,951,000	12,503,871	18,457,000
Elevation (m)	124	25	14	450	2850	126	170	11	7	2640	25	2240
PM_{10}	19.76–146.11	24.8–35.4	25–46	101.09–106.71	24.91–26.13	80–281	32.9–83.2	22.9	73.11–83.52	41.42–52.04	48	19–174
Al	0.18–3.28	0.67–1.13	0.455–1.13	0.078–0.1	0.382–0.913	–	0.0329–0.0832	0.427	0.59–0.70	0.898–1.107	–	–
Mg	0.12–0.41	0.29–0.40	–	–	1.556–1.894	–	–	0.803	0.34–0.82	0.105–0.138	–	–
Ca	0.23–3.65	0.51–1.81	–	3.88–3.93	6.552–7.809	–	–	2.997	1.57–2.17	1.082–1.534	–	–
Ba	0.11–0.15	–	0.022–0.043	0.22–0.257	0.138–0.242	–	–	–	–	–	–	–
Na	–	–	–	–	3.910–4.786	–	–	–	–	0.069–0.125	–	–
Si	1.01–9.19	–	–	17.804–25.949	0.196–0.255	–	–	–		3.290–4.121	–	–
Fe	0.29–4.75	0.32–0.54	0.298–0.83	3.048–3.795	0.363–0.444	0.30–6.17	–	0.994	0.62–0.86	0.663–1.068	0.086	0.0007–0.0033
S	–	0.87–0.96	–	0.276–0.292	1.014–1.207	–	–	–	–	–	–	–
Zn	0.08–0.51	–	0.017–0.060	0.032–0.064	0.0651–0.1213	0.2–1.630	–	0.039	0.13–0.46	0.037–0.194	0.027	0.032–0.210
V	0.0–0.03	–	0.010–0.022	0.016–0.017	0.005–0.010119	–	0.0037–0.0095	0.005	4.46–5.15	–	–	0.002–0.029
Pb	0.01–0.03	–	0.0098–0.020	0.003–0.013	0.0196–0.023854	0.070–1.030	0.0254–0.0711	–	62.75–100.52	–	0.048	0.0001–0.0009
Ni	0.01–0.02	–	0.0037–0.008	0.004–0.006	0.0028–0.0147	0.040–0.270	0.0092–0.0159	–	8.27–9.58	–	0.004	0.0006–0.007
Mn	0.02–0.08	–	0.0066–0.018	0.073–0.088	0.03110–0.0417	–	0.0044–0.0211	0.014	20.62–26.08	0.005–0.020	–	0.0008–0.0042
Cr	–	–	0.0031–0.0093	0.008	0.009258–0.0954	0.032–0.4	–	–	4.97–6.85	0.007	–	0.0002–0.0008
Cu	0.11–0.24	–	0.0099–0.083	0.011–0.027	0.05351–0.20007	–	0.013–0.141	0.087	15.33–63.53	0.013–0.028	0.007	0.005–0.041
Cd	–	–	–	–	0.001522–0.0029	0.002–0.043	0.0019–0.0037	–	–	–	–	–
NH_4^+	3.11–7.96	0.50	–	–	0.068–0.155	–	–	–	3.05–3.31	0.276–0.360	2.6	0.01–25.5
NO_3^-	4.73–17.29	0.72–0.77	–	–	0.332–0.398	–	–	–	4.45–5.29	0.744–1.117	4.1	1.4–4.3
SO_4^{2-}	1.76–6.67	2.31–2.39	–	–	2.340–3.223	–	–	–	14.23–15.90	0.763–1.037	6.8	2.6–7.9

[a] (Morera et al., 2018).
[b] (Celis et al., 2004).
[c] (Dongarrà et al., 2007).
[d] (Lopez et al., 2011).
[e] (Bogo et al., 2003).
[f] (Sharma and Maloo, 2005).
[g] (Manalis et al., 2005).
[h] (Loyola et al., 2012).
[i] (Ho et al., 2003).
[j] (Vargas et al., 2012).
[k] (Gutierez-Castillo et al., 2005).
[l] Present work.

sources in this city, such as soil, as well as meteorological conditions that could promote the resuspension of dust in this city. In addition, the city is rapidly growing, with an intense activity of constructions, especially in the central Site 1 - Belisario and the area near Site 3 - Tababela. Most of the other elements are well compared with all other cities, except for S concentration, which is mainly formed from burning of coal (Braga et al., 2004). Its concentration is higher in Quito if compared to other two reported cities (Cienfuegos (Cuba) and Cordoba (Argentina)), which could be explained by the low-quality high sulfur content fuels (Zalakeviciute et al., 2017) used in a more populous city. This may imply serious health risks for the population of this rapidly growing city.

Table 5 shows that the concentrations of the inorganic ions NO_3^- and SO_4^{2-}, which are formed from the oxidation of pollutants associated with combustion emissions, i.e., NO_x and SO_2, respectively, are well compared with other developing countries. This suggests that the implementation of stricter regulations to reduce combustion emissions is necessary in the city of Quito. On the other hand, the concentration of NH_4^+, which is mainly derived from agriculture activities, i.e. NH_3, and acidic species present in either the gas or aerosol phase, is at least twice lower in Quito than in the other cities.

Finally, it can be observed in Table 5 that there is no direct relation between the concentration of PM_{10} and population or elevation. For example, the PM_{10} concentration in Quito (2,239,191 inhab., 2850 m.a.s.l.) is comparable to the concentrations found in Cienfuegos (150,404 inhab., 25 m.a.s.l.), Palermo (673,735 inhab., 14 m.a.s.l) and even in Rio de Janeiro (6,320,446 inhab., 11 m.a.s.l.). On the other hand, the cities with the highest PM_{10} concentrations were Chillan (146,701 inhab. 124 m.a.s.l.), Cordoba (1,391,000 inhab., 450 m.a.s.l.), Kanpur (2,715,555 inhab., 126 m.a.s.l.) and Mexico City (18,457,000 inhab., 2240 m.a.s.l.). It might suggest that there are several other variables, different than the population and elevation that influence the overall PM_{10} concentrations in a city, such as meteorology, terrain, topography, fuel availability, etc.

For instance, in a previous study we showed the positive impact of implementations of fuels and traffic regulations on air quality (Zalakeviciute et al., 2017). This advocates studies focusing on cities of all population sizes, since in many cases, a smaller city may also have air pollution problems (see Table 5).

An additional correlation analysis shows the coefficients of correlation between the concentration of PM_{10} and the groups of the chemical elements and demographic/geographic data, after a normalization based on the value of PM_{10} (Table 6). A positive correlation is observed between the traffic-related elemental fraction and the elevation of the city (R = 0.76). Different factors may influence this behavior. For example, the decrease in air pressure and shortage of oxygen concentration in the air of high altitude cities can change the normal operation of the engine, i.e., can increase the fuel consumption and decrease the thermal efficiency (Wang et al., 2013), can reduce the power output (He et al., 2011) and can deteriorate the in-cylinder combustion (Liu et al., 2017). As a result, the vehicle exhaust emissions can be promoted (Bishop et al., 2001; Rech et al., 2007; Wang et al., 2018). Also, the complexity of terrain, common in high elevation cities (included in this study), can affect the vehicle emissions, as it might involve more braking and more accelerating. To the best of our knowledge, these studies do not exist, suggesting opportunities for posible future investigations. Similarly, a positive correlation between the traffic tracers in PM_{10} and the year is observed (R = 0.51), possibly because of the motorization tendency in the world (Bureau of Transportation Statistics, 2019). On the other hand, a significant positive correlation between population and industrial tracers is observed (R = 0.70), which suggests that the increase in population might consequently augment the fraction of industrial composition of PM_{10} (Peterson, 1973).

Table 6
Pearson correlation of the normalized parameters for 12 representative cities in the world: Cienfuegos (Cuba), Chillan (Chile), Cordoba and Buenos Aires (Argentina), Rio de Janeiro (Brazil), Bogota (Colombia), Mexico City (Mexico), Palermo (Italy), Athens (Greece), Kanpur (India), Hong Kong (China), and Quito (Ecuador). In bold, high correlation coefficients are shown.

Demographic/geographic information	PM_{10}	Sources			
		Natural	Traffic	Mixed	Industrial
Year	−0.45	0.34	0.51	−0.42	−0.46
Population	0.05	−0.48	0.38	0.34	**0.7**
Elevation	−0.21	−0.03	**0.76**	−0.07	0.29

4. Conclusions

The first ever PM_{10} chemical analysis was performed in the high elevation complex terrain Ecuadorian capital – Quito. The analysis of PM_{10} elements and inorganic ions was successfully carried out during the first ten months of 2017 in three different sites of the city. Average PM_{10} concentrations varied from 24.9 $\mu g\,m^{-3}$ to 26.2 $\mu g\,m^{-3}$, with some peaks during episodes of fires and New Year's festivities. The major chemical elements found in all the studied sites were Ca, Na, S, Mg, P, K, Fe, Si and Al, representative of natural sources of soil and dust resuspension. Central Site 1 - Belisario, differs by higher concentrations of Zn, B, Ba, Cr, Sr, Mn, As, Ni and Cd, associated with anthropogenic, mostly, traffic-related emissions. In developing countries, low quality diesel fuel is recognized for emitting higher quantities of heavy metals, resulting in increased levels of those tracers in traffic circulated areas. Southern valley Site 2 - Los Chillos showed higher concentrations of Cu and V, compared with the other two sites, which are metals related to industrial activities. Finally, the most rural Site 3 - Tababela presented higher values for natural tracers Al, Mg and Ca, compared to the other two sites. Factor analysis showed a mix between the anthropogenic and natural sources for this site, suggesting dust saturation with transported urban pollution. Some tracer metals for airport emissions (Ba, Pb, Cr and Zn) were also registered in this site. The most abundant inorganic ion in Quito was SO_4^{2-}, indicating combustion of fossil fuels and industrial activities.

A comparison of the results obtained in this work, with those of other cities, showed that the elevation of the city could be an important contributing factor for traffic tracer emissions. The air quality in relatively small population size Quito compares well with other cities of the world, with the presence of high concentrations of some toxic metals hazardous to human health such as Cr. Concentrations of this toxic metal exceed health recommendations by up to 475 times, with peaks attributed to firework activity. This implies the necessity of stricter regulations in some cities, whether it has to do with firework use or control on their quality. Another health violation is shown for Ni and As concentrations and annual PM_{10} levels.

This work emphasizes the fact that megacities are not necessarily the only ones suffering from air pollution. This suggests that more attention should be given to midsize cities that lack stricter regulations. This problem constitutes a fundamental challenge in terms of public health, since the continued exposure to PM and toxic compounds can yield adverse effects in the long term, especially in children and elderly. In that sense, this study paves the way for further research to better understand the air quality in midsize high elevation cities.

Declaration of competing interest

Authors state that there are no conflicts of interest.

Acknowledgements

This research was done in collaboration with Secretariat of the Environment of Quito, Ecuador. The funding was provided by

Universidad de Las Americas, Ecuador, as part of two research projects AMB.RZ.17.06 and AMB.RZ.19.01. Authors are very grateful to Dr. David R. Sannino for proofreading for English language.

Appendix A. Supplementary data

Supplementary data to this article can be found online at https://doi.org/10.1016/j.apr.2019.11.007.

References

Aguilera Sammaritano, M., Bustos, D.G., Poblete, A.G., Wannaz, E.D., 2017. Elemental composition of PM 2.5 in the urban environment of San. Environ. Sci. Pollut. Res.

Aldabe, J., Elustondo, D., Santamaría, C., Lasheras, E., Pandol, M., Alastuey, A., Querol, X., Santamaría, J.M., 2011. Chemical characterisation and source apportionment of PM2.5 and PM10 at rural , urban and traf fi c sites in Navarra (North of Spain), vol. 102. pp. 191–205. https://doi.org/10.1016/j.atmosres.2011.07.003.

Almeida, T.S., Sant Ana, M.O., Cruz, J.M., Tormen, L., Frescura Bascunan, V., Azevedo, P.A., Garcia, C., Alves, J., Araujo, R., 2017. Characterisation and source identification of the total airborne particulate matter collected in an urban area of Aracaju, Northeast, Brazil. Environ. Pollut. https://doi.org/10.1016/j.envpol.2017.04.018.

Anderson, L.D., Faul, K.L., Paytan, A., 2010. Phosphorus associations in aerosols : what can they tell us about P bioavailability? Mar. Chem. 120, 44–56. https://doi.org/10.1016/j.marchem.2009.04.008.

Bei, N., Zhao, L., Wu, J., Li, X., Feng, T., Li, G., 2018. Impacts of sea-land and mountain-valley circulations on the air pollution in Beijing-Tianjin-Hebei (BTH): a case study. Environ. Pollut. 234, 429–438. https://doi.org/10.1016/j.envpol.2017.11.066.

Belis, C.A., Karagulian, F., Larsen, B.R., Hopke, P.K., 2013. Critical review and meta-analysis of ambient particulate matter source apportionment using receptor models in Europe. Atmos. Environ. 69, 94–108. https://doi.org/10.1016/j.atmosenv.2012.11.009.

Bishop, G.A., Morris, J.A., Stedman, D.H., Cohen, L.H., Countess, R.J., Countess, S.J., Maly, P., Scherer, S., 2001. The effects of altitude on heavy-duty diesel truck on-road emissions. Environ. Sci. Technol. 35, 1574–1578. https://doi.org/10.1021/es001533a.

Bogo, H., Otero, M., Castro, P., Ozafrán, M.J., Kreiner, A., Calvo, E.J., Negri, R.M., 2003. Study of atmospheric particulate matter in Buenos Aires city. Atmos. Environ 37, 1135–1147. https://doi.org/10.1016/S1352-2310(02)00977-9.

Boyle, K.A., 1996. Evaluating particulate emissions from jet engines: analysis of chemical and physical characteristics and potential impacts on coastal environments and human health. Transp. Res. Rec. 1517, 1–9. https://doi.org/10.3141/1517-01.

Braga, C.F., Teixeira, E.C., Yoneama, M.L., Dias, J.F., 2004. Study of the elemental composition of aerosols in the Candiota region of Brazil using the PIXE technique. Nucl. Instrum. Methods Phys. Res. Sect. B Beam Interact. Mater. Atoms 225, 561–571. https://doi.org/10.1016/j.nimb.2004.05.023.

Braga, C.F., Teixeira, E.C., Meira, L., Wiegand, F., Yoneama, M.L., Dias, J.F., 2005. Elemental composition of PM10 and PM2.5 in urban environment in South Brazil. Atmos. Environ 39, 1801–1815. https://doi.org/10.1016/j.atmosenv.2004.12.004.

Bravo Alvarez, H., Sosa Echeverria, R., Sanchez Alvarez, P., Krupa, S., 2013. Air quality standards for particulate matter (PM) at high altitude cities. Environ. Pollut. 173, 255–256. https://doi.org/10.1016/j.envpol.2012.09.025.

Bureau of Transportation Statistics, 2019. World motor vehicle production, selected countries (thousands of vehicles. [WWW Document]. United States Dep. Transp. URL. https://www.bts.gov/bts/archive/publications/national_transportation_statistics/table_01_23, Accessed date: 15 September 2019.

Cazorla, M., 2016. Air quality over a populated andean region: insights from measurements of ozone, NO, and boundary layer depths. Atmos. Pollut. Res. 7, 66–74. https://doi.org/10.1016/j.apr.2015.07.006.

Celis, J., Morales, R., Zaror, C.A., Inzunza, J.C., 2004. A study of the particulate matter PM10 composition in the atmosphere of Chillan, Chile. Chemosphere 54, 541–550. https://doi.org/10.1016/S0045-6535(03)00711-2.

Cevallos, V.M., Diaz, V., Sirois, C.M., 2017. Particulate matter air pollution from the city of Quito, Ecuador, activates inflammatory signaling pathways in vitro. Innate Immun. 23, 392–400. https://doi.org/10.1177/1753425917699864.

Chen, L.C., Lippmann, M., 2009. Effects of metals within ambient air particulate matter (PM) on human health. Inhal. Toxicol. 21, 1–31. https://doi.org/10.1080/08958370802105405.

Dai, Q.L., Bi, X.H., Wu, J.H., Zhang, Y.F., Wang, J., Xu, H., Yao, L., Jiao, L., Feng, Y.C., 2015. Characterization and source identification of heavy metals in ambient PM10 and PM2.5 in an integrated Iron and Steel industry zone compared with a background site. Aerosol Air Qual. Res. 15, 875–887. https://doi.org/10.4209/aaqr.2014.09.0226.

Ding, J., Zhu, T., 2003. Heterogeneous reactions on the surface of fine particles in the atmosphere. Chin. Sci. Bull. 48, 2267–2276. https://doi.org/10.1360/03wb0046.

Do, T., Wang, C., Hsieh, Y., Hsieh, H., 2012. Metals present in ambient air before and after a firework festival in Yanshui, Tainan, Taiwan. Aerosol Air Qual. Res. 3, 981–993. https://doi.org/10.4209/aaqr.2012.03.0069.

Dong, Q., Zhao, P.-S., Wang, Y.-C., Miao, S.-G., Gao, J., 2017. Impact of mountain-valley wind circulation on typical cases of air pollution in Beijing. Huanjing Kexue 38, 2218–2230. https://doi.org/10.13227/j.hjkx.201609231.

Dongarrà, G., Manno, E., Varrica, D., Vultaggio, M., 2007. Short communication. Atmos. Environ. 41, 7977–7986. https://doi.org/10.1016/j.atmosenv.2007.09.015.

Du, B., Wei, Q., Wang, S., Yu, W., 1997. Application of microemulsions in determination of chromium naphthenate in gasoline by flame atomic absorption spectroscopy. Talanta 44, 1803–1806. https://doi.org/10.1016/S0039-9140(97)00053-2.

EMASEO, 2011. Municipio del distrito metropolitano de Quito: Plan de Desarrollo 2012–2022. Quito.

EPA, 1997. 4-108 Inorganic Nonmetals (4000): 4500-NH3 NITROGEN (AMMONIA) Method. pp. 108–117.

EPA, 2000. Ultraviolet Spectrophotometric Screening Method 4500-NO3. pp. 120–129.

Estrella, B., Sempértegui, F., Franco, O.H., Cepeda, M., Naumova, E.N., 2018. Air pollution control and the occurrence of acute respiratory illness in school children of Quito, Ecuador. J. Public Health Policy. https://doi.org/10.1057/s41271-018-0148-6.

Fergusson, J.E., Kim, N.D., 1991. Trace elements in street and house dusts: sources and speciation. Sci. Total Environ. 100, 125–150. https://doi.org/10.1016/0048-9697(91)90376-P.

Phantom Fireworks, 2019. Chem. Compd No Title [WWW Document]. https://fireworks.com/education-and-safety/chemistry-compounds.

Fordyce, J.S., Sheibley, D.W., 1975. Estimate of contribution of jet aircraft operations to trace element concentration at or near airports. J. Air Pollut. Control Assoc. 25, 721–724. https://doi.org/10.1080/00022470.1975.10470131.

Gibb, H.J., Lees, P.S.J., Pinsky, P.F., Rooney, B.C., 2000. Lung cancer among workers in chromium chemical production. Am. J. Ind. Med. 38, 115–126. https://doi.org/10.1002/1097-0274(200008)38:2<115::AID-AJIM1>3.0.CO;2-Y.

Greven, F.E., Vonk, J.M., Fischer, P., Duijm, F., Vink, N.M., Brunekreef, B., 2019. Air pollution during New Year's fireworks and daily mortality in The Netherlands. Sci. Rep. 9, 5735. https://doi.org/10.1038/s41598-019-42080-6.

Guerrero-Latorre, L., Romero, B., Bonifaz, E., Timoneda, N., Rusiñol, M., Girones, R., Rios-touma, B., 2018. Science of the Total Environment Quito's virome: metagenomic analysis of viral diversity in urban streams of Ecuador's capital city. Sci. Total Environ. 645, 1334–1343.

Gutierez-Castillo, M.E., Olivos-Ortiz, M., De Vizcaya-Ruiz, A., Cebrian, M.E., 2005. Chemical characterization of extractable water soluble matter associated with PM 10 from Mexico City during 2000. Chemosphere 61, 701–710. https://doi.org/10.1016/j.chemosphere.2005.03.063.

Harris, A.M., Sempértegui, F., Estrella, B., Narváez, X., Egas, J., Woodin, M., Durant, J.L., Naumova, E.N., Griffiths, J.K., 2011. Air pollution and anemia as risk factors for pneumonia in ecuadorian children: a retrospective cohort analysis. Environ. Health 10, 93. https://doi.org/10.1186/1476-069X-10-93.

He, C., Ge, Y., Ma, C., Tan, J., Liu, Z., Wang, C., Yu, L., Ding, Y., 2011. Emission characteristics of a heavy-duty diesel engine at simulated high altitudes. Sci. Total Environ. 409, 3138–3143. https://doi.org/10.1016/j.scitotenv.2011.01.029.

Ho, K.F., Lee, S.C., Chan, C.K., Yu, J.C., Chow, J.C., Yao, X.H., 2003. Characterization of chemical species in PM2.5 and PM10 aerosols in Hong Kong. Atmos. Environ. 37, 31–39.

Iijima, A., Sato, K., Yano, K., Tago, H., Kato, M., Kimura, H., Furuta, N., 2007. Particle size and composition distribution analysis of automotive brake abrasion dusts for the evaluation of antimony sources of airborne particulate matter. Atmos. Environ. 41, 4908–4919. https://doi.org/10.1016/j.atmosenv.2007.02.005.

INEC, 2011. Poblacion, superficie (km2), densidad poblacional a nivel parroquial. Quito.

INEC-DMTV, 2019. Proyecciones de población del Distrito Metropolitano de Quito al 2020. Densidad de población por parroquia. [WWW Document]. Mapas Relac. - Proyecciones población del Dist. Metrop. Quito al 2020. URL. https://www.gifex.com/detail/2011-10-26-14684/Proyecciones_de_poblacion_del_Distrito_Metropolitano_de_Quito_al_2020.html, Accessed date: 4 September 2019.

James, K.A., Strand, M., Hamer, M.K., Cicutto, L., 2018. Health services utilization in asthma exacerbations and PM10 levels in rural Colorado. Ann. Am. Thorac. Soc. 15, 947–954. https://doi.org/10.1513/AnnalsATS.201804-273OC.

Jia, M., Zhao, T., Cheng, X., Gong, S., Zhang, X., Tang, L., Liu, D., Wu, X., Wang, L., Chen, Y., 2017. Inverse Relations of PM2.5 and O3 in air compound pollution between cold and hot seasons over an urban area of East China. Atmosphere 8, 1–12. https://doi.org/10.3390/atmos8030059.

Kai, Z., Yuesi, W., Tianxue, W., Yousef, M., Frank, M., 2007. Properties of nitrate, sulfate and ammonium in typical polluted atmospheric aerosols (PM10) in Beijing. Atmos. Res. 84, 67–77. https://doi.org/10.1016/j.atmosres.2006.05.004.

Karagulian, F., Belis, C.A., Dora, C.F.C., Prüss-Ustün, A.M., Bonjour, S., Adair-Rohani, H., Amann, M., 2015. Contributions to cities' ambient particulate matter (PM): a systematic review of local source contributions at global level. Atmos. Environ. 120, 475–483. https://doi.org/10.1016/j.atmosenv.2015.08.087.

Korn, M. das G.A., dos Santos, D.S.S., Welz, B., Vale, M.G.R., Teixeira, A.P., Lima, D. de C., Ferreira, S.L.C., 2007. Atomic spectrometric methods for the determination of metals and metalloids in automotive fuels–a review. Talanta 73, 1–11. https://doi.org/10.1016/j.talanta.2007.03.036.

Li-Jones, X., Prospero, J.M., 1998. Variations in the size distribution of non-sea-salt sulfate aerosol in the marine boundary layer at Barbados: impact of African dust. J. Geophys. Res. Atmos. 103, 16073–16084.

Licudine, J.A., Yee, H., Chang, W.L., Whelen, A.C., 2012. Hazardous metals in ambient air due to new year fireworks during 2004-2011 celebrations in Pearl City, Hawaii. Public Health Rep. 127, 440–450. https://doi.org/10.1177/003335491212700412.

Liu, J., Ge, Y., Wang, X., Hao, L., Tan, J., Peng, Z., Zhang, C., Gong, H., Huang, Y., 2017. On-board measurement of particle numbers and their size distribution from a light-duty diesel vehicle: influences of VSP and altitude. J. Environ. Sci. (China) 57, 238–248. https://doi.org/10.1016/j.jes.2016.11.023.

López, J.M., Callén, M.S., Murillo, R., García, T., Navarro, M.V., De La Cruz, M.T., Mastral, A.M., 2005. Levels of selected metals in ambient air PM10 in an urban site of Zaragoza (Spain). Environ. Res. 99, 58–67. https://doi.org/10.1016/j.envres.2005.01.007.

Lopez, M., Ceppi, S., Palancar, G.G., Olcese, L.E., Tirao, G., Toselli, B.M., 2011. Elemental concentration and source identification of PM10 and PM2.5 by SR-XRF in Córdoba City, Argentina. Atmos. Environ. Times 45, 5450–5457. https://doi.org/10.1016/j.atmosenv.2011.07.003.

Lough, G.C., Schauer, J.J., Park, J.S., Shafer, M.M., Deminter, J.T., Weinstein, J.P., 2005. Emissions of metals associated with motor vehicle roadways. Environ. Sci. Technol. 39, 826–836. https://doi.org/10.1021/es048715f.

Loyola, J., Arbilla, G., Quiterio, S.L., Escaleira, V., Minho, A.S., 2012. Trace metals in the urban aerosols of Rio de Janeiro city. J. Braz. Chem. Soc. 23, 628–638.

Manalis, N., Grivas, G., Protonotarios, V., Moutsatsou, A., Samara, C., Chaloulakou, A., 2005. Toxic metal content of particulate matter (PM10), within the Greater Area of Athens. Chemosphere 60, 557–566. https://doi.org/10.1016/j.chemosphere.2005.01.003.

Martínez-España, R., Bueno-Crespo, A., Timón, I., Soto, J., Muñoz, A., Cecilia, J.M., 2018. Air-pollution prediction in smart cities through machine learning methods: a case of study in Murcia, Spain. J. Univers. Comput. Sci. 24, 261–276.

Molina, M.J., Molina, L.T., Molina, M.J., Molina, L.T., 2016. Megacities and Atmospheric Pollution Megacities and Atmospheric Pollution, vol. 2247https://doi.org/10.1080/10473289.2004.10470936.

Moreda-Piñeiro, J., Turnes-Carou, I., Alonso-Rodríguez, E., 2015. The influence of oceanic air masses on concentration of major ions and trace metals in PM2.5 fraction at a coastal European suburban site. Water Air Soil Pollut. 226–2240. https://doi.org/10.1007/s11270-014-2240-2.

Morera, Y., Elustondo, D., Lasheras, E., Alonso, C.M., Miguel, J., 2018. Chemical characterization of PM10 samples collected simultaneously at a rural and an urban site in the Caribbean coast: local and long-range source apportionment. Atmos. Environ. 192, 182–192. https://doi.org/10.1016/j.atmosenv.2018.08.058.

Pastrana-Corral, M.A., Wakida, F.T., Temores-Peña, J., Rodriguez-Mendivil, D.D., García-Flores, E., Piñon-Colin, T.D.J., Quiñonez-Plaza, A., 2017. Heavy metal pollution in the soil surrounding a thermal power plant in Playas de Rosarito, Mexico. Environ. Earth Sci. 76. https://doi.org/10.1007/s12665-017-6928-7.

Peterson, E.W., 1973. Interaction of population growth, industrial growth and pollution control. J. Air Pollut. Control Assoc. 23, 11–16.

Pope, C.A., Dockery, D.W., 2006. Health effects of fine particulate air Pollution : lines that connect. Air Waste Manag. Assoc. 56, 709–742. https://doi.org/10.1080/10473289.2006.10464545.

Pöschl, U., 2005. Atmospheric chemistry atmospheric aerosols: composition, transformation, climate and health effects. Angew. Chem. Int. Ed. 44, 7520–7540. https://doi.org/10.1002/anie.200501122.

Queiroz Aucelio, R., Curtius, A.J., 2002. Evaluation of electrothermal atomic absorption spectrometry for trace determination of Sb, as and Se in gasoline and kerosene using microemulsion sample introduction and two approaches for chemical modification. J. Anal. At. Spectrom. 17, 242–247. https://doi.org/10.1039/B108928P.

Querol, X., Alastuey, A., Ruiz, C.R., Artin, B., Hansson, H.C., Straehl, P., Schneider, J., 2004. Speciation and origin of PM10 and PM2.5 in selected European cities, vol. 38. pp. 6547–6555. https://doi.org/10.1016/j.atmosenv.2004.08.037.

Querol, X., Viana, M., Alastuey, A., Amato, F., Moreno, T., Castillo, S., Pey, J., Rosa, J. De, Sa, A., Salvador, P., Santamarı, J.M., Zabalza, J., 2007. Source origin of trace elements in PM from regional background. Urban Ind. Sites Spain 41, 7219–7231. https://doi.org/10.1016/j.atmosenv.2007.05.022.

Quiroz, W., Cortés, M., Astudillo, F., Bravo, M., Cereceda, F., Vidal, V., Lobos, M.G., 2013. Antimony speciation in road dust and urban particulate matter in Valparaiso, Chile: analytical and environmental considerations. Microchem. J. 110, 266–272. https://doi.org/10.1016/j.microc.2013.04.006.

Quiterio, S.L., Sousa da Silva, C.R., Arbilla, G., Escaleira, V., 2004. Metals in airborne particulate matter in the industrial district of Santa Cruz, Rio de Janeiro, in an annual period. Atmos. Environ. 38, 321–331. https://doi.org/10.1016/j.atmosenv.2003.09.017.

Ramírez, O., Sánchez de la Campa, A.M., de la Rosa, J., 2018. Characteristics and temporal variations of organic and elemental carbon aerosols in a high–altitude, tropical Latin American megacity. Atmos. Res. 210, 110–122. https://doi.org/10.1016/j.atmosres.2018.04.006.

Raysoni, A.U., Armijos, R.X., Margaret Weigel, M., Echanique, P., Racines, M., Pingitore, N.E., Li, W.W., 2017. Evaluation of sources and patterns of elemental composition of PM2.5 at three low-income neighborhood schools and residences in Quito, Ecuador. Int. J. Environ. Res. Public Health 14, 1–26. https://doi.org/10.3390/ijerph14070674.

Rech, C., Leamar, R., Blanco, D., Flach, M.A., 2007. Sae Technical Paper Series 2007-01-2632.

Riojas-Rodriguez, H., da Silva, A.S., Texcalac-Sangrador, J.L., Moreno-Banda, G.L., 2016. Air pollution management and control in Latin America and the Caribbean: implications for climate change. Rev. Panam. Salud Públic 40, 150–159.

Ríos-Touma, B., Acosta, R., Prat, N., 2014. The Andean Biotic Index (ABI): revised tolerance to pollution values for macroinvertebrate families and index performance evaluation. Ecol. Freshw. 62, 249–273.

Rotatori, M., Guerriero, E., Sbrilli, A., Confessore, L., Bianchini, M., Marino, F., Petrillt, L., Allegrini, I., 2003. Characterisation and evaluation of the emissions from the combustion of orimulsion-400, coal and heavy fuel oil in a thermoelectric power plant. Environ. Technol. 24, 1017–1023. https://doi.org/10.1080/09593330309385640.

Rybarczyk, Y., Zalakeviciute, R., 2016. Machine learning approach to forecasting urban pollution. In: 2016 IEEE Ecuador Technical Chapters Meeting, ETCM 2016, https://doi.org/10.1109/ETCM.2016.7750810.

Sadiq, M., Alam, I., El-Mubarek, A., Al-Mohdhar, H.M., 1989. Preliminary evaluation of metal pollution from wear of auto tires. Bull. Environ. Contam. Toxicol. 42, 743–748. https://doi.org/10.1007/BF01700397.

Saint'Pierre, T., Maranhão, T.D.A., Frescura, V.L., Curtius, A.J., Aucélio, R.Q., 2008. Determination of Cd and Pb in fuel ethanol by filter furnace electrothermal atomic absorption spectrometry. Quim. Nova 31, 1626–1630.

Sánchez-Ccoyllo, O.R., de Fátima Andrade, M., 2002. The influence of meteorological conditions on the behavior of pollutants concentrations in São Paulo, Brazil. Environ. Pollut. 116, 257–263. https://doi.org/10.1016/S0269-7491(01)00129-4.

Sharma, M., Maloo, S., 2005. Assessment of ambient air PM10 and PM2.5 and characterization of PM10 in the city of Kanpur, India. Atmos. Environ. 39, 6015–6026. https://doi.org/10.1016/j.atmosenv.2005.04.041.

Shen, Z., Sun, J., Cao, J., Zhang, L., Zhang, Q., Lei, Y., Gao, J., Huang, R.J., Liu, S., Huang, Y., Zhu, C., Xu, H., Zheng, C., Liu, P., Xue, Z., 2016. Chemical profiles of urban fugitive dust PM2.5 samples in Northern Chinese cities. Sci. Total Environ. 569–570, 619–626. https://doi.org/10.1016/j.scitotenv.2016.06.156.

Silva, J., Rojas, J., Norabuena, M., Molina, C., Toro, R.A., Leiva-guzmán, M.A., 2017. Particulate matter levels in a South American megacity: the metropolitan area of Lima-Callao , Peru. Environ. Monit. Assess. 189, 635. https://doi.org/10.1007/s10661-017-6327-2.

Smolders, E., Degryse, F., 2002. Fate and effect of zinc from tire debris in soil. Environ. Sci. Technol. 36, 3706–3710. https://doi.org/10.1021/es025567p.

Squizzato, S., Cazzaro, M., Innocente, E., Visin, F., Hopke, P.K., Rampazzo, G., 2017. Urban air quality in a mid-size city — PM2.5 composition, sources and identification of impact areas: from local to long range contributions. Atmos. Res. 186, 51–62. https://doi.org/10.1016/j.atmosres.2016.11.011.

Stanek, L.W., Brown, J.S., Stanek, J., Gift, J., Costa, D.L., 2011. Air pollution toxicology — a brief review of the role of the science in shaping the current understanding of air pollution health risks. Toxicol. Sci. 120, 8–27. https://doi.org/10.1093/toxsci/kfq367.

Steinhauser, G., Sterba, J.H., Foster, M., Grass, F., Bichler, M., 2008. Heavy metals from pyrotechnics in new years eve snow. Atmos. Environ. 42, 8616–8622. https://doi.org/10.1016/j.atmosenv.2008.08.023.

Sternbeck, J., Sjödin, Å., Andréasson, K., 2002. Metal emissions from road traffic and the influence of resuspension - results from two tunnel studies. Atmos. Environ. 36, 4735–4744. https://doi.org/10.1016/S1352-2310(02)00561-7.

Thorpe, A., Harrison, R.M., 2008. Sources and properties of non-exhaust particulate matter from road traffic: a review. Sci. Total Environ. 400, 270–282. https://doi.org/10.1016/j.scitotenv.2008.06.007.

Tsai, J., Lin, J., Yao, Y., Chiang, H., 2012. Size distribution and water soluble ions of ambient particulate matter on episode and non-episode days in Southern Taiwan. Aerosol Air Qual. Res. 12, 263–274. https://doi.org/10.4209/aaqr.2011.10.0167.

United Nations, 2019. Country profiles [WWW Document]. World Urban. Prospect. 2018. URL. https://population.un.org/wup/Country-Profiles/, Accessed date: 9 February 2019.

Vargas, F.A., Rojas, N.Y., Pachon, J.E., Russell, A.G., 2012. PM10 characterization and source apportionment at two residential areas in Bogota. Atmos. Pollut. Res. 3, 72–80. https://doi.org/10.5094/APR.2012.006.

Ventura, L.M.B., Amaral, B.S., Wanderley, K.B., Godoy, J.M., Gioda, A., 2014. Validation method to determine metals in atmospheric particulate matter by inductively coupled plasma optical emission spectrometry. J. Braz. Chem. Soc. 25, 1571–1582. https://doi.org/10.5935/0103-5053.20140142.

Viana, M., Querol, X., Götschi, T., Alastuey, A., Sunyer, J., Forsberg, B., Heinrich, J., Norbäck, D., Payo, F., Maldonado, J.A., Künzli, N., 2007. Source apportionment of ambient PM2.5 at five Spanish centres of the european community respiratory health survey (ECRHS II). Atmos. Environ. 41, 1395–1406. https://doi.org/10.1016/j.atmosenv.2006.10.016.

Viana, M., Pandolfi, M., Minguillón, M.C., Querol, X., Alastuey, A., Monfort, E., Celades, I., 2008. Inter-comparison of receptor models for PM source apportionment: case study in an industrial area. Atmos. Environ. 42, 3820–3832.

Villalobos, A.M., Barraza, F., Jorquera, H., Schauer, J.J., 2015. Chemical speciation and source apportionment of fine particulate matter. Sci. Total Environ. 512–513, 133–142. https://doi.org/10.1016/j.scitotenv.2015.01.006.

Wang, X., Ge, Y., Yu, L., Feng, X., 2013. Effects of altitude on the thermal efficiency of a heavy-duty diesel engine. Energy 59, 543–548. https://doi.org/10.1016/j.energy.2013.06.050.

Wang, H., Ge, Y., Hao, L., Xu, X., Tan, J., Li, J., Wu, L., Yang, Jia, Yang, D., Peng, J., Yang, Jin, Yang, R., 2018. The real driving emission characteristics of light-duty diesel vehicle at various altitudes. Atmos. Environ. 191, 126–131. https://doi.org/10.1016/j.atmosenv.2018.07.060.

Watson, J.G., Chow, J.C., 2001. Source characterization of major emission sources in the Imperial and Mexicali Valleys along the US/Mexico border. Sci. Total Environ. 276, 33–47.

WHO, 2014. 7 million premature deaths annually linked to air pollution. [WWW Document]. Media Cent. URL. http://www.who.int/mediacentre/news/releases/2014/air-pollution/en/#.WqBfue47NRQ.mendeley, Accessed date: 3 July 2018.

Wrzesinsky, T., Klemm, O., 2000. Summertime fog chemistry at a mountainous site in central Europe. Atmos. Environ. 34, 1487–1496. https://doi.org/10.1016/S1352-2310(99)00348-9.

Xiao, Z.M., Zhang, Y.F., Hong, S.M., Bi, X.H., Jiao, L., Feng, Y.C., Wang, Y.Q., 2011. Estimation of the main factors influencing haze, based on a long-term monitoring campaign in Hangzhou, China. Aerosol Air Qual. Res. 11, 873–882. https://doi.org/10.4209/aaqr.2011.04.0052.

Yangyang, X., Bin, Z., Lin, Z., Rong, L., 2015. Spatiotemporal variations of PM2.5 and PM10 concentrations between 31 Chinese cities and their relationships with SO2, NO2, CO and O3. Particuology 20, 141–149. https://doi.org/10.1016/j.partic.2015.01.003.

Yao, X., Chan, C.K., Fang, M., Cadle, S., Chan, T., Mulawa, P., He, K., Ye, B., 2002. The water-soluble ionic composition of PM2.5 in Shanghai and Beijing, China. Atmos. Environ. Times 36, 4223–4234. https://doi.org/10.1016/S1352-2310(02)00342-4.

Young, T.M., Heeraman, D.A., Sirin, G., Ashbaugh, L.L., 2002. Resuspension of soil as a source of airborne lead near industrial facilities and highways. Environ. Sci. Technol. 36, 2484–2490. https://doi.org/10.1021/es015609u.

Zalakeviciute, R., Alexander, M.L., Allwine, E., Jimenez, J.L., Jobson, B.T., Molina, L.T., Nemitz, E., Pressley, S.N., Vanreken, T.M., Ulbrich, I.M., Velasco, E., Lamb, B.K., 2012. Chemically-resolved aerosol eddy covariance flux measurements in urban Mexico City during MILAGRO 2006. Atmos. Chem. Phys. 12. https://doi.org/10.5194/acp-12-7809-2012.

Zalakeviciute, R., Rybarczyk, Y., López-Villada, J., Diaz Suarez, M.V., 2017. Quantifying decade-long effects of fuel and traffic regulations on urban ambient PM2.5 pollution in a mid-size South American city. Atmos. Pollut. Res. https://doi.org/10.1016/j.apr.2017.07.001.

Zalakeviciute, R., López-Villada, J., Rybarczyk, Y., 2018. Contrasted effects of relative humidity and precipitation on urban PM2.5 pollution in high elevation urban areas. Sustainability 10, 2064. https://doi.org/10.3390/su10062064.

Zhou, J., Xing, Z., Deng, J., Du, K., 2016. Characterizing and sourcing ambient PM2.5 over key emission regions in China I: water-soluble ions and carbonaceous fractions. Atmos. Environ. 135, 20–30. https://doi.org/10.1016/j.atmosenv.2016.03.054.